# ASSESSING SENSOR-MODEL-FUSION TECHNOLOGIES ON A FLEXIBLE AEROELASTIC WING DEMONSTRATOR THROUGH WIND TUNNEL TESTING IN THE DLR PROJECT SAFER<sup>2</sup>

T. G. Schmidt\*, R. Volkmar, B. Micheli, F. Stalla, R. Konatala, C. Hanke\*, A. Altkuckatz\*, L. Koida\*, M. Braune\*, K. Soal\*, M. Tang\*, M. Böswald\*, J. Dillinger\*, Y. Boose<sup>†</sup>, H. Mai<sup>§</sup>

\* German Aerospace Center (DLR), Institute of Aeroelasticity, Göttingen, Germany

† German Aerospace Center (DLR), Institute of Lightweight Systems, Braunschweig, Germany

§ German-Dutch Wind Tunnels (DNW), Marknesse, The Netherlands

#### **Abstract**

This study discusses the experimental exploration of novel sensor-model-fusion technologies on a flexible aeroelastic wing demonstrator through wind tunnel testing, as part of the DLR project SAFER<sup>2</sup>. The aeroelastic wing demonstrator is excited via inflow gusts and disturbances, generated by a gust rig, or using control surface deflections. A large variety of sensor systems are employed to capture these excitations and measure the loads, thereby enabling the effective testing of sensor-model-fusion technologies. Among the latter, active control methods to alleviate gust loads and to augment the wing damping, as well as an online-monitoring framework to identify structural modal parameters are explored. Two gust load alleviation strategies are investigated, which are either based on a robust control approach or leverage reinforcement learning techniques. The online-monitoring framework implements various operational modal analysis methods, coupling them with a linear Kalman filter. The damping augmentation controller uses a destabilization/stabilization approach, featuring a novel input-output blending method as well as a saturation mechanism to guarantee a safe operation. All sensor-model-fusion technologies tested yield promising results, whether these concern the effective reduction of gust-induced loads (e.g., wing-root bending moment), the accurate online monitoring of modal parameters, or the controlled destabilization and re-stabilization of the wing model using damping augmentation.

## **Keywords**

Aeroelastic Wind Tunnel Testing, High-Aspect-Ratio Wing Configuration, Sensor-Model-Fusion; Gust Load Alleviation; Damping Augmentation; Operational Modal Analysis

# 1. INTRODUCTION

There is a worldwide push within the aerospace industry towards developing more efficient aircraft, with the objective to reduce their emissions and, thus, their ecological footprint. This calls for modern propulsion technologies, aircraft fuels, and design concepts as well as pushing the boundaries of those that already exist. For instance, high-aspect-ratio wing (HARW) configurations constitute one promising solution to reach higher aerodynamic efficiency and thus lower fuel consumption. Compared to existing designs, such slender and lightweight wings are more prone to experience adverse aeroelastic phenomena (e.g., unsteady structural loads, limit-cycle oscillations (LCO), flutter). To counteract these phenomena, a common approach is to monitor and eventually mitigate them using active control, which can enhance the aircraft's operational safety without the need for excessively stiff and heavy airframes. For traditional sensing-and-control strategies, which rely on isolated measurements and specific analytical models, it may be more challenging to capture the nonlinear dynamics inherent to such flexible wing structures, often leading to more conservative designs or delayed mitigation actions. Recent advances in sensor-model (data) fusion - combining dense, multimodel sensor streams (e.g., surface pressures, accelerations, loads and moments) with data-driven algorithms such as deep learning, Kalman-filter variants, and physicsinformed neural networks - may offer a way to extract latent state information, predict impending aeroelastic events, and enable proactive control actuation. The efficacy of such fusion frameworks, however, needs to be rigorously validated under controlled yet realistic aerodynamic loading conditions, including - but not limited to - variations in inflow speeds, angles, and disturbances (e.g., gusts). Hence, experimental campaigns on representative test models are necessary. These challenges are explored within the DLR project "Sensor and Al Fusion for Enhanced Peformance and Reliability" (or SAFER2), in which various DLR institutes come together to investigate their respective sensor-model-fusion technologies on five technology demonstrators, among which a flexible aeroelastic

wing which is focus of the present paper. The sensormodel-fusion strategies explored include the real-time online monitoring of structural modal parameters as well as control algorithms aiming at augmenting the structural damping or alleviating gust loads.

This paper is structured as follows: The aeroelastic wing demonstrator is introduced in Section 2 before the experimental setup and means used throughout the measurement campaigns are discussed (see Section 3). Next, Sections 4, 5, and 6 respectively introduce one of the sensor-model-fusion technologies tested within the SAFER<sup>2</sup> project, providing methodology, objectives, and some preliminary results. Finally, some conclusions and perspectives are provided in Section 7.

## 2. AEROELASTIC WING DEMONSTRATOR

The aeroelastic wing demonstrator is based upon the geometry of the wing model developed within the optimal Load-Adaptive aircraFt (oLAF) project [1], whose reference aircraft is a wide-body long-range configuration, with a wingspan of 57.7 m (i.e., an aspect ratio of roughly 10) thus representing a HARW type. For more details on this aircraft configuration, the reader is referred to [2-5]. While the aeroelastic wing demonstrator adopts the oLAF models aerodynamic shape and structural design, overall, it differs by a few key characteristics; First, the aeroelastic wing demonstrator features four trailing-edge flaps that are located over the outboard part of the wing. Second, the aeroelastic wing demonstrator comprises a larger amount and higher variability of sensors, which is pivotal for the effective testing of sensor-model-fusion technologies. An overview of the wing planform along with its sensors' location is shown in Fig. 1.

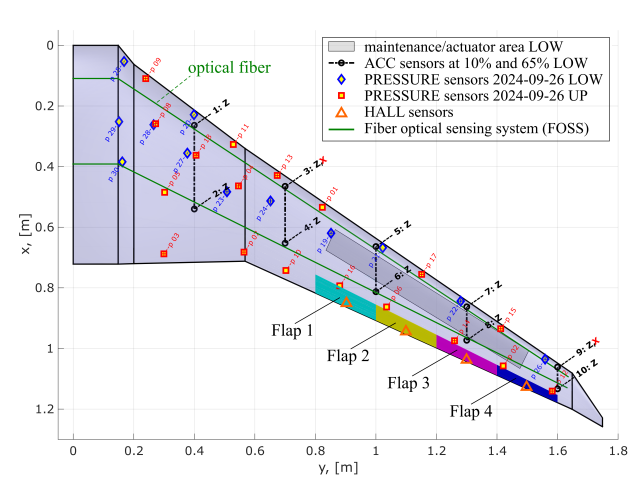


FIG 1. Sensor and actuator positions on the planform of the aeroelastic wing demonstrator

The demonstrator features 30 unsteady pressure sensores, of which 18 and 12 are located on the wing's suction and pressure side, respectively. In addition, 12 acceleration sensors are installed, with ten of those measuring the acceleration in vertical (z) direction and two capturing the streamwise (x)

direction. To better monitor the wing's elastic deformation due to control surface deflections and gust encounters, a fiber-optical sensor system (FOSS) is implemented [6], which consists of four optical fibers embedded inside the model covers, two on each side. This allowed for a realistic strain signal over the whole length of the fibers, which run from root to tip. Strain measurements are then obtained via an Optical Distributed Sensor Interrogator (ODiSI) system, which determines local strain by sending infrared light through the optical fibers and evaluating the differences in wavelength and runtime of the backscattered light. Spatial resolutions of the FOSS of 1.3 mm and 2.6 mm are used. To capture the trailing-edge flaps deflections, hall sensors located on each flap hinge are implemented. Finally, the global aerodynamic forces and moments are obtained by a 6-component piezo-electric balance, to which the demonstrator's root is mounted on.

### 3. EXPERIMENTAL SETUP

The experimental test campaigns within the SAFER² project are conducted within the DNW-NWB, a low-speed wind tunnel of Göttinger type, i.e., closed-loop (see Fig. 2), which is located at the DLR site in Braunschweig and operated by the German-Dutch Wind Tunnels (DNW). The wind tunnel features a closed-vein test section of dimensions 3.25 m (W) × 2.8 m (H) × 8.0 m (L) whose inflow can reach mean speeds of  $U_{\infty}$  = 0 - 90 m/s at low turbulence levels of Ti < 0.06%.

To generate inflow gusts, a gust rig consisting of four units, each of which featuring an airfoil vane and a rotating slotted cylinder, is specifically designed for the DNW-NWB test section (its preliminary two-unit setup being discussed in detail in [7]). The rig is mounted on sets of grooved aluminum panels upstream of the aeroelastic wing demonstrator, thereby allowing the units' position to be varied in lateral and streamwise directions (if desired). Each cylinder is driven by a high-performance brushless DC motor with an integrated encoder, which is operated via an in-house developed control software. The built-in encoder as well as externally mounted reflex light barrier are used to monitor and regulate the cylinders' rotational speed. In addition, the control software features several operational modi that allow for various rotation types, e.g., different continuous and discrete actuations that in turn would result in continuous sinusoidal inflow gusts, discrete "1-cos"-like gust events, or flow disturbances like passive turbulence. The rotational speed can be varied between 0 and 12 Hz, which enables the specific tuning of the inflow gust's signal. To capture the inflow characteristics generated by the gust rig an unsteady fast-response 5-hole pressure probe is mounted on the wind tunnel ceiling, above the demonstrator. The experimental setup used throughout the test campaigns is depicted in Fig. 3.

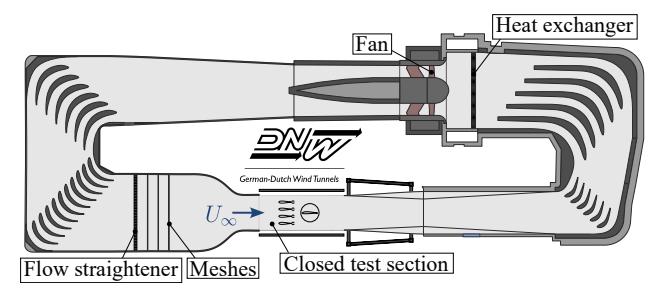


FIG 2. Schematic of the low-speed wind tunnel DNW-NWB



FIG 3. Image of the experimental setup in the test section of the DNW-NWB

The experimental data are measured via several data acquisition (DAQ) systems; a Dewetron measurement system is used with a Dewesoft online monitoring platform (cf. Fig. 4-top), alongside a Simcenter SCADAS hardware and IMC DAQ system (see e.g., Fig. 4-bottom). The sensor signals are split to the various DAQ systems. Even though the SCADAS hardware can be used as a DAQ device, it is here mainly used for generating actuator signals, which are passed via an ADwin-Pro II real-time system to the wing demonstrator's control surfaces. The developed control algorithms discussed in Sections 4 and 2 are also run on this real-time control system.

# 4. GUST LOAD ALLEVIATION

One active control technique supporting lighter highaspect ratio wing configurations is gust load alleviation (GLA). The idea is to reduce the loads seen by the airframe, especially at the highly loaded wingroot, where the wing is attached to the fuselage. This can be achieved by deflecting the available control surface, adapting the lift generation. The control algorithms can be supplied with measurements from multiple sensors: acceleration, deflection, load measurements, or sensors trying to predict the gust. In



FIG 4. Images of the data monitoring setup used during the experimental tests. Top: Sensor signals of the wing demonstrator via Dewesoft. Bottom: Online operational modal analysis.

any case, the objective of GLA poses a multi-variable problem.

The SAFER<sup>2</sup> experiments were used to investigate two possible approaches to address gust load alleviation: a more conventional robust control method, and a reinforcement learning technique. Both approaches are well-suited for this task, and yield similar results, albeit their methodology being largely different.

## 4.1. Robust Control Approach

Robust control is a model-based, linear, frequency-domain method. Starting point is a mathematical description of the system to be controlled, typically as a transfer function or state-space system. This system has inputs and outputs, representing the relevant relations. For the wind tunnel experiment, these are the trailing edge deflections and gust as inputs, and the sensor measurements as outputs. Now, the control objectives need to be transferred to frequency-domain description, by imposing weighting filters on the systems inputs and outputs. This allows to use the  $H_{\infty}$ -norm between the weighted inputs and outputs as an optimization criterion. Aim is the minimization of this norm. Comprehensive details on the robust control method are given in [8–10].

The setup for the GLA problem is presented in Fig. 5. The performance objective are defined on the signal of wing-root bending and torsion moment, denoted p. Additionally, the control activity u and sensor usage v is constrained. External inputs are the gust disturbance d and the noise n. The feedback loop is closed over sensors and control commands to the trailing edge flaps.

In the wind tunnel experiment, multiple sensor signals are provided, see Fig. 1: up to four acceleration sen-

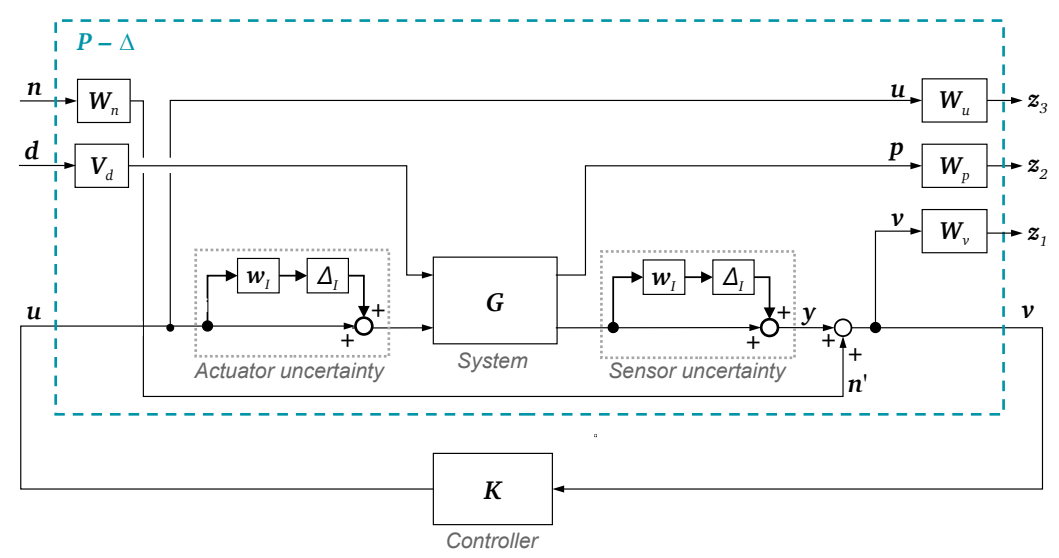


FIG 5. Control architecture for the robust control GLA

sors on the wing (the four closest to the wing tip), and a measurement of the forces and moments on the load balance. Four trailing edge control surfaces are available. The robust control approach allows to connect these sensors and actuators in an optimal way, through an unstructured synthesis [8]. Sensor fusion and control allocation tasks are thereby performed during the synthesis, while the weighting functions allow to reflect limitations of the individual sensors and actuators.

An especially intuitive approach to implement sensor and actuator limitations is the extension of  $H_{\infty}$ -based robust control to  $\mu$ -synthesis [11–13], which allows to define uncertainties within the system formulation. Hence, properties like sensor bias, sensor noise, or flap effectiveness can be included in the problem formulation, and are taken into account during the controller design. In Fig. 5 the uncertainty is represented as a structured multiplicative uncertainty at the actuators (input, i) and sensors (output o) [9].

Further details on the  $\mu$ -synthesis development and testing in a similar wind tunnel experiment are given in [14]. In the SAFER² the setup included the feedback of the measured roll moment and lift force at the wing root, besides the four acceleration sensors. The results indicate that the force and moment sensors are more effective in mitigating slow (low-frequency) gusts, while the acceleration sensors perform better near the first flexible eigenfrequency of the wing, where loads are the highest. Through  $\mu$ -synthesis an optimal usage of the available sensors is achieved for all frequencies.

An exemplary result is shown in Fig. 6, for a continuous, sinusoidal gust excitation with 8.5 Hz, which is close to the first flexible eigenfrequency at a wind speed of 30 m/s. The upper plot depicts the reduction in measured wing-root bending moment, the lower plot depicts the related control surface deflection. In the design it was chosen that only the outer two flaps are used for this high-frequency range, while all four flaps are active in the low frequency regime. Hence,

only the outer two flaps are seen moving in the figure.

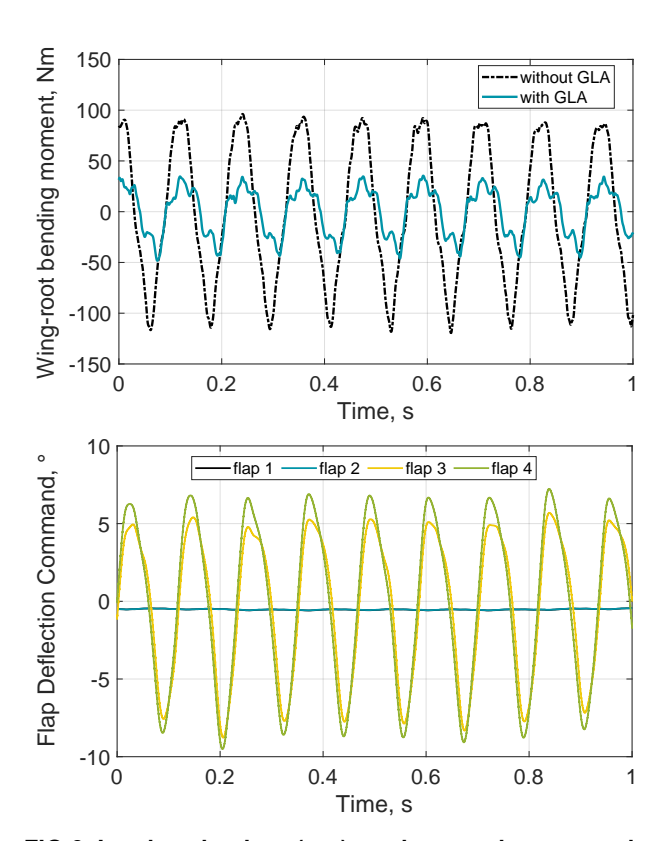


FIG 6. Load reduction (top) and control commands (bottom) for a sinusoidal gust with 8.5 Hz

Besides the load reduction displayed above, also robustness properties are satisfactory. Evaluating the structured singular value  $\mu$  [15] and disk-based margins [16] confirm stability and performance even in the presence of uncertainty. This is important, since the model used for controller design will never entirely match the real experiment.

More details on the robust control approach are given in [14]. Another approach to cope with uncertainties, changing operating conditions, and even nonlinearities in the GLA setting is explored in the following section.

# 4.2. Reinforcement Learning Approach

The increasing structural flexibility of modern aircraft, driven by high aspect-ratio wings and lightweight materials, poses significant challenges for conventional model-based flight control systems. Such systems often struggle to cope with complex, nonlinear aeroelastic interactions and may be limited in adaptability and performance under varying conditions. Therefore, an alternative, model-free control strategy, namely reinforcement learning (RL), is explored. In this context, a Soft Actor-Critic (SAC) based controller has been developed to alleviate gust loads on the aeroelastic wing demonstrator. The approach leverages offline training with simulation data and wind tunnel configurations to design a controller that learns directly from sensor feedback without requiring an explicit aeroelastic model. The aeroelastic wing demonstrator integrates state-of-the-art sensing and actuation, enabling closed-loop validation of the SAC controller under realistic gust conditions. This GLA method contributes to objective in SAFER2 of validating intelligent, data-driven control strategies to enhance the performance and reliability of future flexible aircraft.

# 4.2.1. Offline training and simulation results

In this section, the training process of the SAC controller is outlined. The model incorporates structural dynamics, unsteady aerodynamics, actuator dynamics, and multiple sensor inputs to closely reflect the experimental setup. Acceleration measurements from four sensor locations serve as observations, while a single control surface (Flap 4) is used for control actions. A gust disturbance model enabled the simulation of sinusoidal, 1-cos, and chirp-type disturbances, which was used during controller training.

Training was performed on data simulated from a linearized model trimmed at a freestream velocity of 30 m/s, discretized with a 1 ms timestep. The SAC controller showed effective load alleviation across various disturbance scenarios, with chirp-based training providing the best generalization performance. Reward shaping and a high discount factor (0.9999) were essential for stable learning.

# 4.2.2. Experimental evaluation of the SAC Baseline Controller

To validate the SAC baseline controller in a physical environment, wind tunnel tests were performed at a freestream velocity of 30 m/s, with sinusoidal gusts in the 6–12 Hz range, encompassing the wing's first bending mode near 8.5 Hz.

Even though the wing features four independently actuated trailing-edge flaps, for these tests, only the outermost flap (Flap 4) was used in the control loop. The SAC controller operated in this single-actuator

configuration, relying on acceleration sensor feedback and actuator position measurements from hall sensors. A real-time supervisory system monitored operating limits, such as excessive accelerations. If limits were exceeded, the actuators were frozen at their current positions, gradually returned to neutral, and the controller was disengaged to ensure safe recovery.

Each test followed a structured sequence: 10 s of open-loop gust excitation, 20 s of closed-loop operation with Flap 4 active, and a final 10s of open-loop flight. This procedure allowed direct comparison between open- and closed-loop responses, providing a systematic evaluation of the controller's effectiveness. Figure 7 presents the wing root bending moment (WRBM) and Flap 4 deflection for a representative test point, with the right-hand plots showing an expanded view between 7-10s to highlight the effect of the GLA controller. Under the SAC controller, WRBM peak-to-peak is reduced from 200 Nm in open loop to 80 Nm in closed loop, using only one actuator, demonstrating effective gust load alleviation under an 8.5 Hz sinusoidal gust, corresponding to the first bending mode, generated with two gust generators.

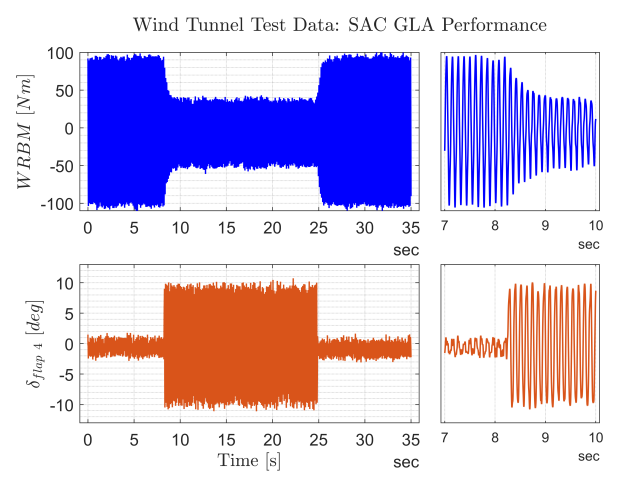


FIG 7. Representative test results of the GLA potential offered by the SAC Baseline Controller

# 5. OPERATIONAL MODAL ANALYSIS

Real-time identification and tracking of eigenfrequencies, damping ratios and mode shapes is a key enabler for safe testing of aeroelastic systems - in wind tunnel or flight testing [17]. Building on the robust online-monitoring framework introduced in [18], the wind-tunnel campaign on the flexible aeroelastic wing demonstrator addresses three tightly coupled research topics:

Broad-band excitation concepts. Three independent sources were employed to generate a rich, non-stationary excitation spectrum: (i) a gust-generator providing impulse-like aerodynamic excitation, (ii) the ambient turbulence of the wind tunnel, and (iii) active control-surface modulation (flap) using four input patterns – repeated

10 ms impulses, band-limited random excitation, logarithmic frequency sweeps and dwells. The different excitation strategies are compared due to their applicability in modal parameter identification in stationary test points as well as a continuously changing wind speed.

2) Comparison of stationary and continuously changing wind speeds. Stationary test conditions for modal parameter identification in aeroelastic applications require significant testing time and result in limited resolution of the flutter curves as can be seen in Fig. 8. Using continuous acceleration of the inflow, more detailed flutter curves are achieved in less time. Nevertheless, assumptions of operational modal analysis - stationary system and excitation - are not fulfilled anymore and lead to increased uncertainties. A detailed comparison of these test approaches is part of the test campaign.

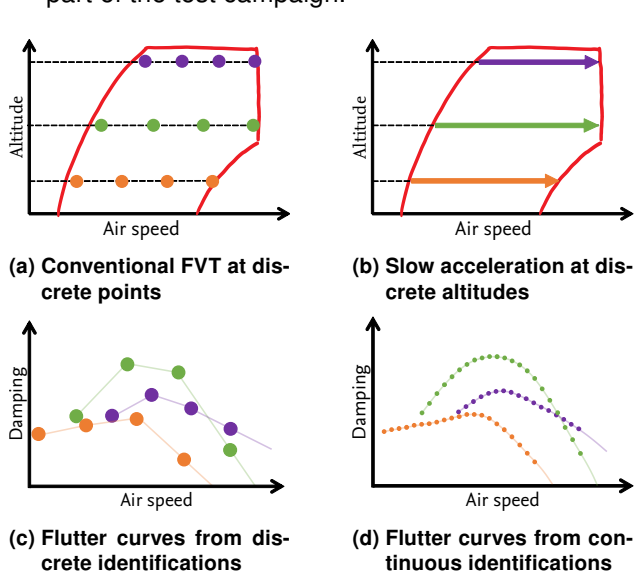


FIG 8. Scheme of FVT procedures and identified flutter curves (taken from [18])

3) Data-fusion based tracking of autonomously identified modal parameters. The measured acceleration signals from accelerometers are processed in 30 s sliding windows with 2 s updates (overlap 93%). Within each window three operational modal analysis (OMA) methods run in parallel: stochastic subspace identification (SSI-COV and SSI-DAT) for time-domain analysis and least-squares complex frequency (LSCF) for frequency-domain analysis. The Automated Modal Analysis (AMA) framework [19] clusters the modal estimates over a range of model orders; the intra-cluster variance provides a qualitative uncertainty for each estimate.

The three estimates (either eigenfrequency f or damping  $\xi$ ) are fed together as measurement input to a linear Kalman filter [17]. An example of the uncertainty reduction using the Kalman filter is shown in Fig. 9. For the sake of simplicity, only SSI is shown here. The uncertainty reduction using

the data fusion based approach will be quantified in this campaign.

## 5.1. Validation and key findings

Reference data were obtained from 2-min stationary recordings at wind speeds of 20, 25, 30, 35, 40, 45 and 50 m/s and analyzed offline using conventional modal analysis. The online fused Kalman estimates achieve comparable accuracy while providing an update every 2 s.

## 5.2. Implications for sensor-model-fusion

The three research topics outlined above are deliberately interlocked: the diverse excitation concepts provide rich data streams; the AMA-based fusion exploits complementary strengths of SSI and LSCF; and the Kalman filter supplies temporal consistency. This integrated framework supplies the online modal parameters required for the destabilize/stabilize approach described in Section 6 (damping-augmentation control).

## 5.3. Open challenges

While the linear constant-rate state model works well for the moderate speed ramps investigated, more abrupt aerodynamic changes (e.g., flow separation) may require higher-order or interacting-multiple-model (IMM) Kalman filters. Moreover, the current uncertainty estimate is based on cluster variance; developing a statistically rigorous, near-real-time uncertainty propagation (e.g., via bootstrap or Bayesian OMA) is a priority for future work.

In summary, the OMA frametwork presented here delivers a compact, robust, and real-time capability to monitor the flexible wing's dynamic behavior. Its seamless integration with the broader SAFER<sup>2</sup> activities makes it a key enabling technology for active aeroelastic control and for the safety of aeroelastic wind-tunnel testing at DLR.

## 6. DAMPING AUGMENTATION CONTROL

The goal of this test is to explore active control technologies that can mitigate aeroelastic instabilities such as flutter or limit cycle oscillations and restore the system stability. Nevertheless, testing an unstable aeroelastic system is still viewed with caution due to the safety implications and potential damages related to a plausible failure of the stabilizing control law.

To provoke an instability during the test in a safe manner, the so-called destabilize/stabilize approach is adopted [20]. This method involves a first control loop that actuates selected control surfaces in a closed-loop configuration to create an aeroservoelastic instability (destabilizing loop). The resulting system is then used for the experimental development of a damping augmentation controller (stabilizing loop).

The activities summarized in this section further develop the destabilize/stabilize approach by introducing two main novelties: i)  $\mathcal{H}_2$ -optimal blending

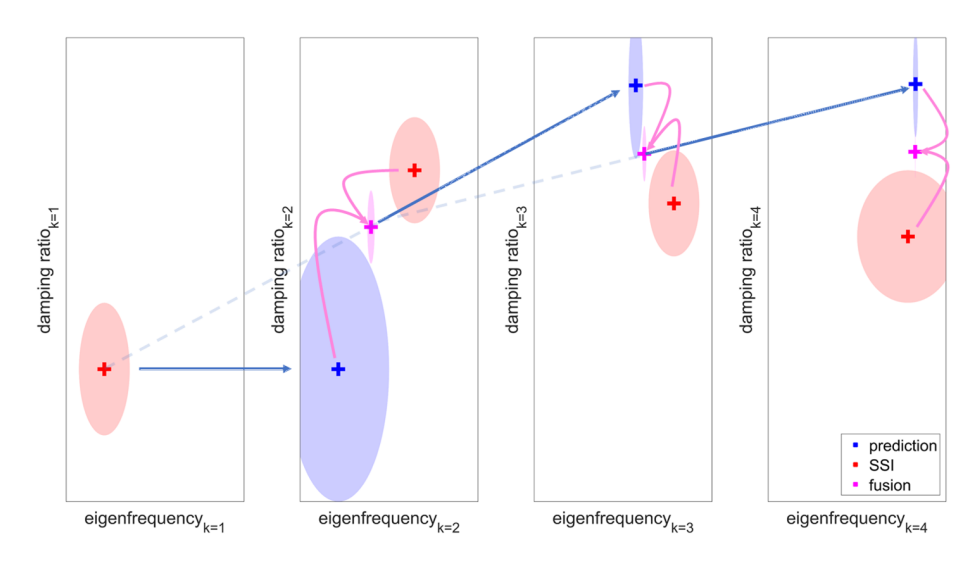


FIG 9. Uncertainty reduction using Kalman filter data fusion of identified modal parameters

of control inputs and measurement outputs [21] is employed for the synthesis of the destabilizing control law. This approach enables isolation of an aeroelastic mode and precise tuning of its aeroelastic damping to a specific value. ii) A saturation block is implemented to limit the action of the destabilizing control surfaces, thereby inducing a limit cycle oscillation when the wing is tested at an unstable configuration. This prevents a divergent response and further increases safety. The scheme of the control architecture is depicted in Fig. 10.

The scheme reveals that only the outermost flap, namely Flap 4, is actuated by the destabilizing loop and that the saturation block is employed to limit its deflections. The blending vectors  $\mathbf{k}_y$  and  $\mathbf{k}_u$ , are designed according to the methods developed by Pusch [21] to isolate the first wing bending mode. The former reads the acceleration measurements a and yields a virtual output  $v_y$  that best represents the response of the target mode. The latter, in this case, corresponds to a unitary gain, as only a single flap is actuated in the loop, which is included in Fig. 10 for completeness.

With the derived blending vectors, the original control problem is transformed into a single-input-single-output (SISO) system. The loop is closed by the SISO controller  $K_{\rm c}(s)$ , whose structure is imposed as  $K_{\rm c}(s)=k_{\rm des}W_{\rm bp}(s)$  where  $W_{\rm bp}(s)$  denotes a 4<sup>th</sup> order Butterworth band-pass filter to avoid interference with steady-state dynamics and noise attenuation, whereas  $k_{\rm des}$  is the static gain to be tuned to affect the aeroelastic damping of the first wing bending mode. This approach had already been adopted during the oLAF project for GLA purposes [22]. Notably, for the GLA application the sign of  $k_{\rm des}$  was reversed as the target was to suppress oscillations instead of to sustain them.

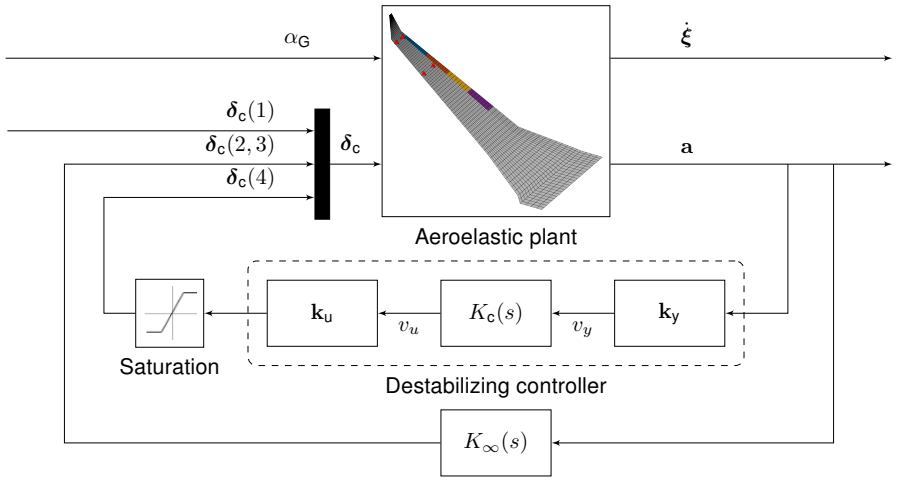
The destabilized wing is afterwards employed for the synthesis of a controller that is able to re-augment the aeroelastic damping, even when  $k_{\text{des}}$  is set to achieve

negative damping values, namely it is set to provoke a deliberate instability. This outer controller, denoted as  $K_{\infty}(s)$  in Fig. 10, is synthesized according to the  $\mathcal{H}_{\infty}$ -control framework for modal damping attenuation presented by Theis et al. [23].

Two primary configurations were examined during the test campaign: one with the stabilizing controller deactivated (OFF) and one with it activated (ON). In both configurations, the destabilizing controller remained active, with the gain  $k_{\rm des}$  adjusted to achieve a set of predefined damping ratios. Specifically, nine discrete values of  $k_{\rm des}$  were tested, corresponding to target damping values  $\zeta_{\rm target} = [10,7,5,3,2,1,0,-1,-2]\%$  according to simulations. The damping augmentation compensator remained unchanged throughout, as it was designed to operate effectively across all configurations defined by the specified  $\zeta_{\rm target}$  values. To validate the controllers, test campaigns were carried out with OMA running in real time to identify and track the modal parameters [17,19,24].

The foremost results are displayed in Fig. 11 along with the numerical predictions; The plot displays the aeroelastic damping of the first wing bending for the nine investigated  $k_{\rm des}$  values, both when the stabilizing controller is deactivated (Stabilizing OFF) and activated (Stabilizing ON). The numerical predictions (solid lines) are compared to the damping identified by real-time OMA (triangular markers). The label "Stabilizing ON SOFT" denotes the case in which the commanded deflection of the stabilizing controller is reduced to 25% before being fed. This measure was adopted as for fully fed deflections (Stabilizing ON FULL) the aeroelastic mode was highly damped, leading to extremely low vibration amplitudes that cannot be identified with OMA anymore [17].

With the destabilizing controller deactivated, numerical predictions showed good agreement with the online OMA measurements. When  $k_{\rm des}$  was tuned to provide -1% and -2% damping, the wing entered a LCO due to the presence of the saturation block. As



Damping augmentation controller

FIG 10. Illustration of the employed closed-loop architecture for damping augmentation activities based on the destabilize/stabilize approach.

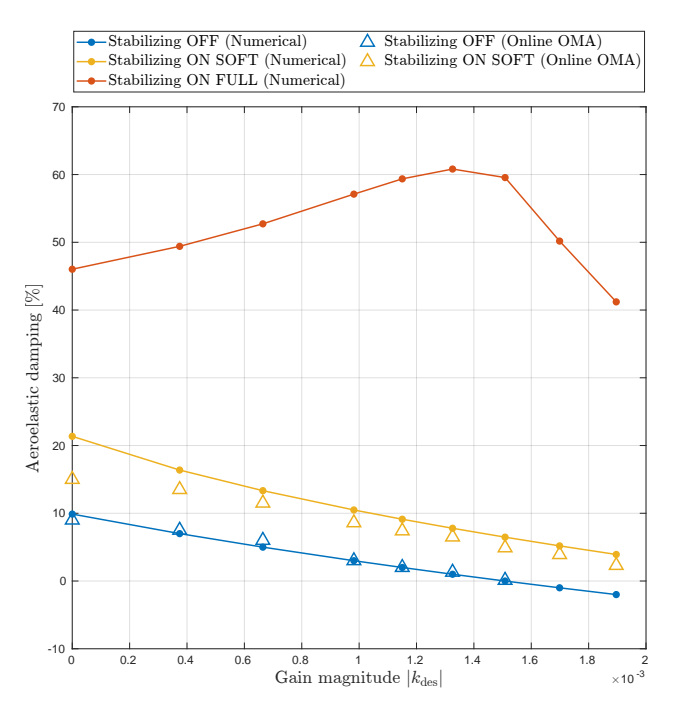


FIG 11. Aeroelastic damping of the first wing bending mode at  $U_{\infty}=50$  m/s under different control configuration.

a result, online OMA reads a sine-like response and identifies zero damping values. These null values are inconsistent with the numerical predictions, and thus the last two data points from the "Online OMA" measurements are intentionally omitted. Nevertheless, the initial wing response, prior to saturation of the destabilizing flap, was divergent, demonstrating that the destabilizing controller successfully provoked the intended instability.

When the stabilizing controller is also activated in full configuration, numerical predictions show a significant increase in damping. The experimental tests confirmed that the wing remained stable across all the investigated gain values, but online OMA loses track of the modes due to the almost absent

vibrations. The action of the stabilizing controller is attenuated to overcome this shortcoming and to validate the aeroelastic system with both control loops operative. Even with the reduced controller active, the system remained stable and a fair comparison between experimental and numerical results is achieved. Specifically, discrepancies are observed at all test points, with the mismatch increasing at higher damping values. This may be related to the fact that, at high damping values, the resulting lower vibration amplitudes reduce the signal-to-noise ratio, thereby increasing the uncertainty in the identification.

The results presented in this section validate the developed  $K_{\infty}(s)$  controller and confirm the potential the destabilizing approach enhanced by the saturation block displays. Finally, the test demonstrates how active damping augmentation control together alongside online OMA can offer significant benefits for applications in future aircraft design.

# 7. CONCLUSIONS

The present study explored several novel sensor-model-fusion technologies, which were experimentally implemented on an aeroelastic wing demonstrator within the wind tunnel tests as part of the DLR project SAFER<sup>2</sup>. More specifically, the aeroelastic wing demonstrator represents a modern, highly flexible, high-aspect-ratio wing configuration, which is equipped with a large number and high variability of sensors and actuators, to facilitate the investigation of such sensor-model-fusion methods. Besides, a gust rig was installed in the test vein to induce inflow gusts and/or flow disturbances, like passive turbulence.

The discussed sensor-model-fusion technologies comprise active control approaches to alleviate gust loads or to augment the wing damping, as well as an online-monitoring framework to identify the wing's structural modal parameters in real-time. Two control approaches aiming at gust load alleviation were

investigated, one based on a robust control and one leveraging reinforcement learning techniques. Both control strategies could offer substantial reductions in the wing loading (e.g., in the wing root bending moment), thereby demonstrating their effective gust load alleviation capabilities. In addition, an operational modal analysis framework was explored, which allows for the compact, robust, and real-time monitoring of the wing's dynamic behavior. Leveraging data fusion techniques, e.g., coupling several operational modal analysis methods together with a linear Kalmnan filter, the modal parameters can be accurately determined in real-time with comparable accuracy as conventional offline analysis. An active control strategy focusing on damping augmentation successfully leveraged a so-called destabilization/stabilization approach, which allows for the careful reduction of the wing damping using one control surface before re-stabilizing the wing using two other flaps. Besides, a saturation block is implemented to limit the destabilizing control surface, to further ensure safe testing. Results showed that the active damping augmentation control together alongside the online operational modal analysis could effectively increase the wing's damping after careful destabilization, thereby representing the promising benefits of such sensor-model-fusion technologies for future aircraft designs.

## Contact address:

tg.schmidt@dlr.de

## References

- [1] Wolf R Krüger, Holger Mai, Thiemo Kier, and Lars Reimer. Assessment of Active Load Control Approaches for Transport Aircraft Simulation and Wind Tunnel Test. In *International Forum on Aeroelasticity and Structural Dynamics, IFASD 2024*, Den Haag, Netherlands, June 2024.
- [2] Matthias Schulze, Thomas Klimmek, Francesco Torrigiani, and Tobias Wunderlich. Aeroelastic Design of the oLAF Reference Aircraft Configuration. In *Deutsche Luft- und Raumfahrtkongress* (DLRK) 2021, page 10, Bremen (virtual), Aug. 2021.
- [3] Matthias Schulze and Vega Handojo. Aeroelastic Design of the oLAF Configuration using Load Alleviation Techniques within cpacs-MONA, Sept. 2023.
- [4] T.F. Wunderlich. Multidisciplinary Optimization of Flexible Wings with Manoeuvre Load Reduction for Highly Efficient Long-Haul Airliners. page 17 pages, 2023. Artwork Size: 17 pages Medium: application/pdf Publisher: Deutsche Gesellschaft für Luft- und Raumfahrt - Lilienthal-Oberth e.V. Version Number: 1.0. DOI: 10.25967/570055.

- [5] Johannes Dillinger, Holger Mai, Wolf R Krüger, Thomas G. Schmidt, and Felix Stalla. Design, Manufacturing and Identification of an Actively Controlled Flexible Wing for Subsonic Wind Tunnel Testing. In *International Forum on Aeroelas*ticity and Structural Dynamics, IFASD 2024, Den Haag, Netherlands, June 2024.
- [6] Erik Kappel, Yannick Boose, Robert Prussak, and Jens Kosmann. On measuring laminate strains of a bent tapered Double-Double panel Comparing strain data from an FE calculation, a high-resolution 3D camera system (ARAMIS) and a fiber-optical sensor system (FOSS). Scientific Report DLR-IB-SY-BS-2023-113, Institute of Lightweight Structures, DLR, Braunschweig, Germany, Aug. 2023.
- [7] Thomas G Schmidt, Johannes Dillinger, Markus Ritter, Anna Altkuckatz, and Marc Braune. Design and Experimental Characterization of a Gust-Generator Concept with Rotating-Slotted Cylinders in the Low-Speed Wind Tunnel DNW-NWB. In International Forum on Aeroelasticity and Structural Dynamics, IFASD 2024, Den Haag, Netherlands, June 2024.
- [8] Sigurd Skogestad and Ian Postlethwaite. Multivariable Feedback Control. John Wiley & Sons, Chichester, UK, 2nd edition edition, 2005. ISBN: 978-0-470-01168-3.
- [9] Kemin Zhou, John C. Doyle, and Keith Glover. Robust and Optimal Control. Prentice Hall, Englewood Cliffs, New Jersey, USA, 2nd edition edition, 1996. ISBN: 978-0-134-56567-5.
- [10] John C. Doyle, Keith Glover, Pramod P. Khargonekar, and Bruce A. Francis. State-Space Solutions to Standard  $H_2$  and  $H_\infty$  Control Problems. *IEEE Transactions on Automatic Control*, 34(8), 1989. DOI:10.1109/9.29425.
- [11] John C. Doyle. Structured Uncertainty in Control System Design. In 24th IEEE Conference on Decision and Control, pages 260–265, Fort Lauderdale, USA, 1985. DOI:10.1109/CDC.1985.268842.
- [12] Gunter Stein and John C. Doyle. Beyond Singular Values and Loop Shapes. *Journal of Guidance*, 14(1), 1991. DOI: 10.2514/3.20598.
- [13] Peter M. Young. Controller Design with Mixed Uncertainties. In *Proceedings of the 1994 American Control Conference ACC*, volume 2, pages 2333–2337, Fort Lauderdale, USA, 1994. DOI: 10.1109/ACC.1994.752496.
- [14] Felix Stalla, Gertjan Looye, Thiemo M. Kier, Kolja Michel, Thomas Schmidt, Charlotte Hanke, Tania Kirmse, and Manuel Pusch. Wind Tunnel Assessment of a Robust Gust Load Alleviation Controller Designed Using  $\mu$ -Synthesis. In

- *AIAA SciTech 2025 Forum*, Orlando, USA, 2025. AIAA. DOI: 10.2514/6.2025-0904.
- [15] John Doyle, Andy Packard, and Kemin Zhou. Review of LFTs, LMIs, and  $\mu$ . In *Proceedings of the 30th IEEE Conference on Decision and Control.*
- [16] Peter Seiler, Andrew Packard, and Pascal Gahinet. An Introduction to Disk Margins [Lecture Notes]. *IEEE Control Systems Magazine*, 40, 2020. DOI: 10.1109/MCS.2020.3005277.
- [17] Robin Volkmar, Julian Sinske, Keith Ian Soal, Yves Govers, and Marc Böswald. Reliable monitoring of modal parameters during a flight vibration test using autonomous modal analysis and a kalman filter. In *International Forum on Aeroelasticity and Structural Dynamics, IFASD 2024*, June 2024.
- [18] Robin Volkmar. Intelligent Modal Analysis System: Autonomous Identification and Tracking of Aircraft Modal Parameters. PhD thesis, Technische Universität Braunschweig, 2025. https://elib.dlr.de/213196/.
- [19] Robin Volkmar, Keith Ian Soal, Yves Govers, and Marc Böswald. Experimental and operational modal analysis: Automated system identification for safety-critical applications. *Mechanical Systems and Signal Processing (MSSP)*, 183(109658), August 2022.
- [20] John K. Berg, Kuang-Ying Ting, Eli Livne, and Kristi Morgansen. Destabilize/stabilize approach to experimental active flutter suppression technology development. *Journal of Guidance, Control, and Dynamics*, 48(5):968–981, 2025. DOI:10.2514/1.G008589.
- [21] Manuel Pusch. Blending of Inputs and Outputs for Modal Control of Aeroelastic Systems. PhD thesis, Technischen Universität Hamburg, November 2020.
- [22] Boris Micheli, Martin Tang, Felix Stalla, Charlotte Hanke, Thomas Schmidt, Holger Mai, and Wolf R. Krueger. Design and Experimental Validation of Gust Load Alleviation Based on H2-Optimal Blending of Inputs and Outputs. DOI:10.2514/6.2025-0901.
- [23] Julian Theis, Harald Pfifer, and Peter Seiler. Robust modal damping control for active flutter suppression. *Journal of Guidance, Control, and Dynamics*, 43(6):1056–1068, 2020. DOI:10.2514/1.G004846.
- [24] Keith Ian Soal, Robin Volkmar, Carsten Thiem, Jan Schwochow, Yves Govers, and Marc Böswald. Identification of the flutter boundary during flight testing using operational modal analysis. In Carlo Rainieri, Carmelo Gentile, and

Manuel Aenlle López, editors, 10th International Operational Modal Analysis Conference, IOMAC 2024, volume 1 of Lecture Notes in Civil Engineering, pages 516–524. Springer, May 2024.